Technical Sciences, 2024, 27, 357–375

UNIWERSYTET WARMIŃSKO-MAZURSKI W OLSZTYNIE

Yearbook peer-reviewed scientific journal
ISSN 1505-4675
e-ISSN 2083-4527
TECHNICAL SCIENCES
Homepage: https://czasopisma.uwm.edu.pl/index.php/ts/

DOI: https://doi.org/10.31648/ts.10111

DEVELOPMENT OF A METHOD FOR ASSESSING THE QUALITY OF BARLEY FOR BREWING USING HYPERSPECTRAL IMAGING

Piotr Zapotoczny

ORCID: 0000-0003-3051-6940
Department of Systems Engineering
University of Warmia and Mazury in Olsztyn

Received 17 April 2024, accepted 29 November 2024, available online 2 December 2024.

K e y w o r d s: vision systems, grain infestation, Fusarium, quality control, hyperspectral image.

A b s t r a c t

The paper discusses the use of hyperspectral imaging in the process of assessing the quality of barley grain intended for brewing purposes. A specialized research set consisting of a spectrophotometer coupled with a CCD camera was used. During the measurements, the spectral distribution of each pixel in the image was recorded in the range of 400 to 1100 nm, which made it possible to extract homogeneous areas on the grain surfaces. Then, surface texture parameters were calculated in the designated areas. Before commencing the classification analyses, the variables were reduced using (a) the Fisher coefficient, (b) the classification error coefficient with the POE+ACC mean correlation coefficient and (c) the mutual information coefficient MI. The best classification results were obtained for the 800 nm wavelength from the isolated homogeneous areas. The accuracy of classification has reached 100% in all quality groups.

Introduction

Contamination of barley grains with *Fusarium* fungi poses a major challenge to malting barley production in most agricultural areas worldwide. The quality of grain is influenced by many factors, including growing conditions, weather,

Correspondence: Piotr Zapotoczny, Katedra Inżynierii Systemów, Wydział Nauk Technicznych, Uniwersytet Warmińsko-Mazurski, ul. Heweliusza 14, 10-718 Olsztyn, e-mail: zap@uwm.edu.pl

harvesting method, and post-harvest storage practices. During storage, the right environmental conditions in the silo, such as the right temperature and humidity levels, as well as ensuring the purity of the grain, are crucial. Grain with increased moisture content after harvest requires appropriate preservative treatments, such as drying and ventilation, to reduce the growth of pathogens and preserve its quality. Optimal storage conditions include grain moisture content of less than 14%, maintaining the right temperature, and eliminating pests such as grain weevils. Ensuring these parameters is crucial to maintaining the safety and utility value of the grain in the long term.

It is important to be able to easily distinguish between high-quality grain and contaminated grain. To achieve this, hyperspectral imaging is increasingly being used. This technique consists in capturing information from the spectrum of electromagnetic radiation in both the visible and invisible range. Its primary advantage is that it leaves the sample intact.

Before the barley grain is used for the malting process, it is necessary to assess its quality, including the distinction between healthy and mould-infested grain, as well as between healthy and rainy grain. Grain infected with fungi is particularly problematic, as it disqualifies the entire batch from further processing. A variety of methods are used to assess quality, such as organoleptic analysis, microbial cultures, genetic techniques (PCR) and visual methods. In recent years, hyperspectral imaging has become increasingly popular, which allows materials to be analyzed using cameras or spectrophotometers in the range of electromagnetic radiation from 200 nm to over 2,500 nm. In particular, far-infrared analysis allows the assessment of the chemical composition, the degree of mold infestation and the damage caused by pests. This method, although extremely precise, is expensive, difficult to implement and limited by a small measurement area, which can lead to unrepresentative results.

In response to these limitations, a new approach to imaging and identification of grain damage was proposed, based on hyperspectral imaging using a spectrophotometer coupled to a CCD camera. This technique allows the spectral distribution of intensity to be recorded for each pixel of the image, generating bitmaps that can be subjected to classic image analysis. This makes it possible to select single wavelengths in the range of 380-1,100 nm, which reveal differences related to fungal infestation or rainfall. This approach is characterized by relatively low implementation costs and simplicity of design, which makes it a promising solution in industrial practice.

Grain quality assessment

Barley is increasingly used in Poland for the production of malt (KAWKA et al. 1998). In order to obtain high-quality malt, barley grain must meet certain quality parameters (GĄSIOROWSKI 1993, p. 19). Methods of assessing the quality of grain are divided into: organoleptic – involving the assessment of grain using the senses of sight, smell, taste and touch. This method does not destroy the sample prepared for analysis, it is fast, but it is not accurate enough. The second group of methods is laboratory

analysis – which involves the study of chemical and physical characteristics that are more complex than organoleptic evaluation and often require expensive, specialized equipment.

Image analysis

The purpose of artificial image processing or analysis is to automatically process and analyze the image of selected objects or the entire environment of an automated system in order to obtain useful information about objects of interest (e.g. those that are subject to manipulation by an industrial robot) or about the environment that may affect the automatically controlled process (TADEUSIEWICZ, KOROHODA 1997). To effectively use an image as a source of information, it is necessary to convert it into a digital image and then carry out an analysis process that includes segmentation, location of objects and determination of their characteristics.

Use of spectral data

Hyperspectral imaging (HSI) is a modern, non-destructive analysis method that allows spectral data to be acquired for each pixel of a sample image. This technology has great potential for the detection of mycotoxins and mycooxygenic fungi in cereals, offering an alternative to time-consuming analytical chemistry methods. Its use can significantly contribute to the reduction of food and feed contamination, as well as the risk of toxic effects on human and animal health. In addition, HSI shows high precision in sorting individual grains, which makes it an effective tool in the selection of bulk materials. In the case of malting barley, it allows you to detect grains that are mouldy, rainy or with a broken germ.

Existing techniques for detecting pathogen infestation in cereals, including high-performance liquid chromatography (HPLC) and enzyme-linked immunosorbent assay (ELISA), are widely used to determine deoxynivalenol (DON) concentrations in wheat. Nevertheless, these methods have their limitations. An ELISA can generate false positive results due to antibody cross-reactivity and false negative results due to low sensitivity (DE GIROLAMO et al. 2009, DOWELL et al. 1999). Chromatography, on the other hand, although extremely precise and selective, is associated with high costs and the need to destroy the sample.

Optical detection techniques, including HSI, have been the subject of intense research in the detection of fungi, especially *Fusarium* species. Many studies focus on the development of classification models that allow for precise differentiation between healthy and damaged grains (DELWICHE et al. 2011, POLDER et al. 2005).

Results indicate that NIR (near-infrared) spectra are more useful in classifying contaminated grains than VIS (visible) spectra. Studies on the characteristics of grain damage caused by *Fusarium* often use visual evaluation as a reference method. Features such as wrinkled surface, pink discoloration, white coating or weight loss are used to identify damaged grains (FDK). For example, DELWICHE and KIM (2000) used a spectral range of 430-860 nm, obtaining a classification accuracy of 86.8-98.4% in two different types of wheat. DELWICHE et al. (2010), on the other hand, obtained 82.5% accuracy of LDA classification by analyzing spectra in the range of 1,000-1,700 nm and combining specific wavelengths such as 1,199 and 1,474 nm.

Further research by DELWICHE et al. (2011) included the use of an additional VIS camera (400-1,000 nm) and new wavelength pairs such as 502 and 678 nm, which resulted in an LDA classification accuracy of 95%. Key findings indicated that pixels originating from the endosperm of the grain provide more useful information compared to those located in the embryo.

HSI technology has been used to detect *Fusarium fungi* in cereals. DELWICHE and KIM (2000) applied a spectral range of 430-860 nm to the analysis of wheat, achieving a classification accuracy of 86.8% to 98.4% depending on the wheat variety. In other studies, DELWICHE et al. (2011) used both VIS (400-1,000 nm) and NIR (1,000-1,700 nm) cameras, which allowed LDA classification accuracy of 95% to be achieved, combining the VIS and NIR bands.

Other studies, such as those conducted by SHAHIN and SYMONS (2011), used the 400-1,000 nm spectral range. Using PCA analysis to select six wavelengths (484, 567, 684, 817, 900, 950 nm), classification accuracy of 92.25% was achieved. SINGH et al. (2012) used artificial grafting with other fungi, such as *Penicillium* and *Aspergillus*, and analyzed only single wavelengths (870 nm), achieving classification accuracy in the range of 88.7-98.0%.

Other examples of research on the use of hyperspectral imaging to determine the degree of fungal infection are the work of SINGH et al. (2007). They used wavelengths in the 1,000 to 1,600 nm range to obtain images of the infected grains. Penicillium fungi were classified with 95% efficiency, while grains infected with A. *niger* and *A. glaucus* were not always classified correctly. Similar work has been carried out by COGDILL et al. (2004), NG et al. (1998), and PERSON and WICKLOW (2006). SINGH et al. (2009) used images taken in the 700-1,100 nm range of infected wheat grains to identify fungi present in Canada. The grains were described using 230 parameters (texture, color, shape). The accuracy of the classification ranged from 95% to 99% depending on the degree of infection and the type/species of pathogen. In a study by BAURIEGEL et al. (2011), infected grain was analyzed using a hyperspectral imaging system in a laboratory setting. Spectral differences between diseased and healthy grain tissues at wavelengths 500-533 nm, 560-675 nm, 682-733 nm and 927-931 nm were used, along with principal component analysis (PCA). The severity of the disease was correctly

classified (87%), taking into account a visual judgment error of 10%. In addition, THOMAS et al. (2017) used hyperspectral imaging to record the genotypes of barley inoculated with *Blumeria graminis f.* sp. *hordei* to characterize the development of the disease

In conclusion, HSI has great potential as a method for the rapid and precise detection of fungal contamination in cereals. Further development of technology and the integration of advanced classification models can significantly improve the processes of sorting and assessing the quality of beans.

Material and methods

Purpose of the study

The aim of the study was to develop a method for identifying malting barley grains infected with pathogens, damaged by rain and healthy using hyperspectral imaging.

Specific objectives:

1. Searching for a wavelength that will allow for the best identification of grains in specific experimental groups.
2. Development of a methodology for segmentation of the grain area, taking into account uniform areas of its surface.
3. Measurement, identification of textures and construction of a statistical model allowing for differentiation of individual experimental groups.

Research methodology

Research material. The research material consisted of spring barley grains of the Sebastian cultivar with a moisture content of 12% (Fig. 1). All grains have been visually classified by the specialist into the following classes:

– healthy;
– rainy,
– infected with fungus.

Healthy malting barley grain has a spindle-shaped shape, light straw color, thin husk and is well uniformed in size, which is conducive to the malting process. Infected grains are characterized by a dark color of varying intensity depending on the degree of fungal infection. Grains damaged by rain also show a dark coloration, but caused by discoloration of the seed coat.

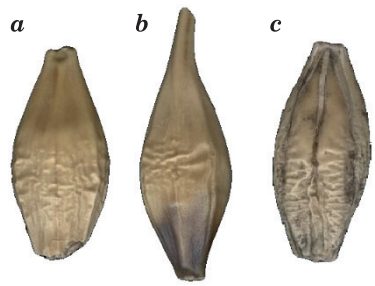

Fig. 1. Images of malting barley kernels:
a – healthy kernels, *b* – black-tipped kernels, *c* – mold-affected kernels

Hyperspectral measurement stand. The test stand has been equipped with a hyperspectral scanner (Fig. 2), a computer and software to control the operating parameters of the *SpecHyp* scanner, such as: image brightness (in the range from 0 to max 255), scanning resolution in the *X* and *Y* axes (*X* 245 mm, *Y* 223 mm) and spectral resolution (0.03 nm). The optical system of the scanner consisted of: UI-1245LE-M-GL camera equipped with a CMOS sensor – Sapphire EV76C560 used to record spatial information, equipped with FL-CC2514-2 lens (focal length 25 mm, aperture F1.4-16), an imaging spectrophotometer, whose task was to divide the light beam into specific lengths and detect the reflected wave from the examined object by the detector. The main source of light was the MI-150 illuminator from Edmund. The images for further analysis were saved in *.bmp, 24-bit format with a resolution of 1024 × 860.

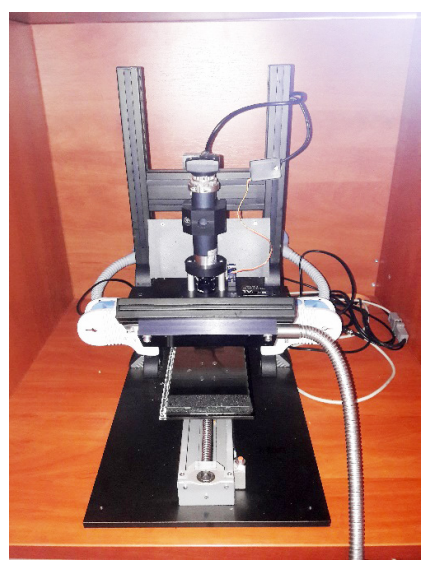

Fig. 2. Hyperspectral scanner

Measurement methodology. Among the obtained grains, samples for testing were identified and manually divided under laboratory conditions into rainy, infected and healthy material. All grains have been numbered and placed in special containers. Then, each grain was scanned from both sides, from the furrow and ridge sides. After setting all the operating parameters, such as spatial and spectral resolution, image brightness and lens magnification, the scan was performed. The view of the scanned grain is shown in Figure 3.

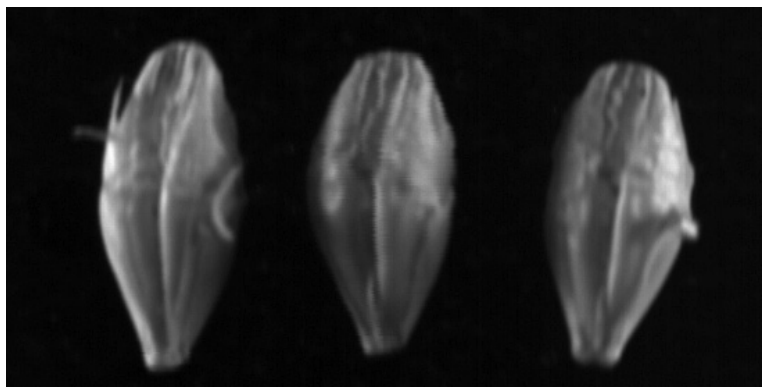

Fig. 3. Scanned grains at the hyperspectral station

100 pcs. of kernels from each class, then randomly divided into two groups: test and teaching in a 40:60 ratio, and additionally 40 pieces were randomly collected. of kernels from each experimental group in order to check the correctness of classification by the discriminant model

SpectraPlugIn software was used to analyse the scanned images, which allows the images in individual spectral channels to be viewed. This functionality allows for visual assessment of the homogeneity of areas and selection of images from spectral channels that potentially show high classification power in the context of further analysis. The choice of channels was made on the basis of visual evaluation of the images of the kernels obtained in the wavelength range of 380-1,100 nm. The selection criterion was the number of details visible in the image in a given channel. In some spectral ranges, the surface texture of the kernels was uniform, which could limit the ability to identify characteristics important for the correct classification of kernels into appropriate classes. Sample images taken for wavelengths of 400, 500, 600, 700 and 800 nm are shown in Figure 4.

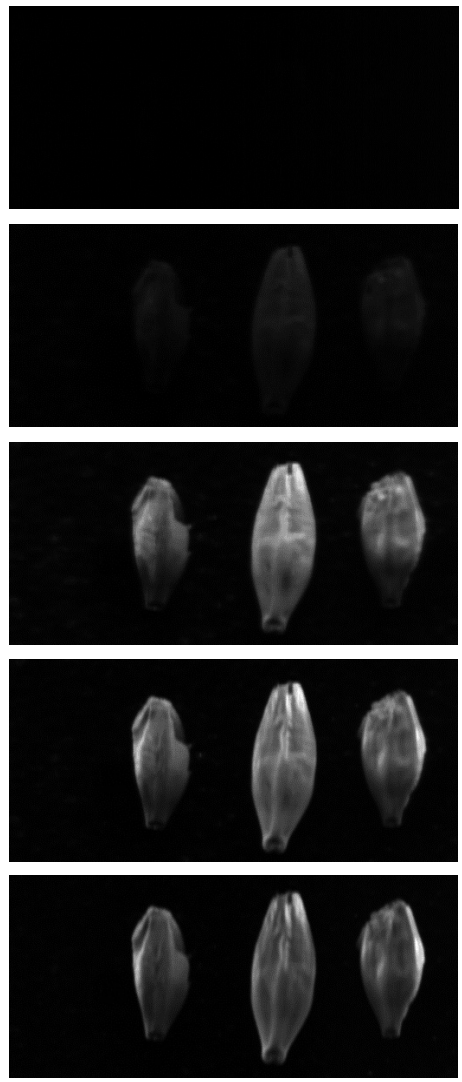

Fig. 4. Photos of the grain taken at wavelengths of 400, 500, 600, 700 and 800 nm

Finally, two wavelengths were selected for further analysis, which contained as much detail as possible on the surface of the kernels – 600 and 800 nm. 6 experimental groups were obtained for each wavelength:

– healthy grains – ventral side – 600 nm (H_V_600);
– healthy grains – dorsal side – 600 nm (H_D_600);
– rained grains – dorsal side – 600 nm (B_D_600);
– rained grains – ventral side – 600 nm (B_V_600);

– infected grains – dorsal side – 600 nm (M_D_600);
– infected grains – ventral side – 600 nm (M_V_600).

Further analysis included the use of classical methods of image segmentation on bitmap data, including:

– determination of the binarization threshold to separate objects from the background;
– determination of the threshold for joining uniform areas on the surface of the corresponding grain side and determination of the number of these areas.

The main goal of this stage was to generate useful masks, so-called *Regions of Interest* (ROIs), representing areas of the grain surface with a uniform texture. Differential correlation analysis was used to identify uniform areas, which allowed precise control of the number of isolated regions by adjusting the value of the correlation coefficient. As part of the analysis, the division of the kernel surface into 3, 4, 5 and 6 uniform ROI areas was studied, adjusting the number of segments to the specific textural properties of the samples. An example of the division into 4 classes of homogeneous areas is shown in Figure 5.

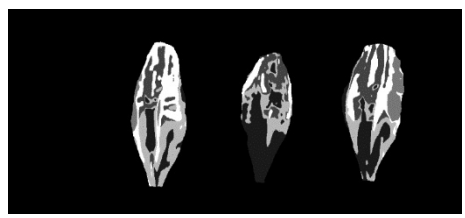

Fig. 5. View of scanned grains after segmentation for 4 homogeneous areas

On the basis of the analysis of the obtained images, it was decided to use the division into three areas (Fig. 6) in further analysis. It was considered that such a division would enable efficient calculation of textural parameters, which in turn should contribute to the development of an effective classification model. This decision was also justified by the opinions of specialists in organoleptic assessment, who indicated that the division into smaller, more detailed areas may make it difficult to correctly identify the assignment of kernels to a specific

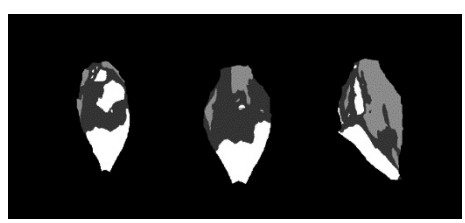

Fig. 6. View of scanned grains after segmentation for 3 homogeneous areas

quality class. Such a division is consistent with both the requirements of the analytical method and the subjective criteria of expert evaluation, which further emphasizes its legitimacy in the context of the analysis.

After segmentation, the obtained areas were converted into 1-bit masks (ROI file) used in the next stage of analysis. The next step was to apply an image mask to the original 24-bit image and then calculate the features describing the image texture for a given area (Fig. 7). The MaZda program was used to calculate the textures of the image (SZCZYPIŃSKI 2010).

After calculating the textural parameters, a final report was generated, containing numerical values describing each analysed area. The final stage of the study was the statistical analysis of the results, which consisted of two key steps: reduction of the number of variables and classification analysis.

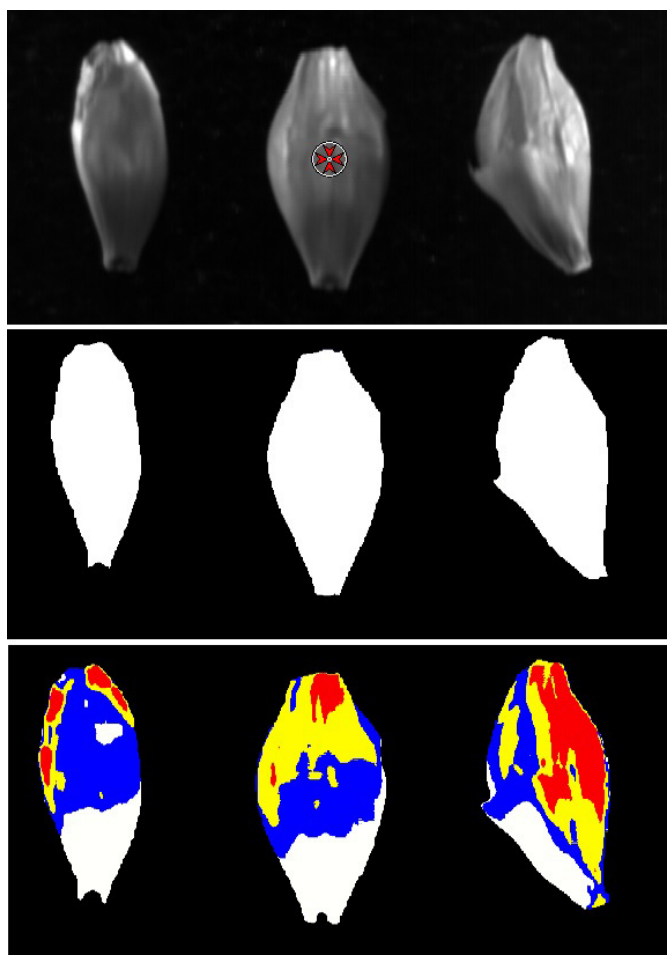

Fig. 7. View of grains after segmentation into 3 areas and their binary masks

In order to carry out the discriminant analysis, ten variables with the highest discriminatory strength were selected. The multivariate analysis was carried out using Statistica v.13 software, using a stepwise discriminant analysis, in which the criterion for introducing the next variable into the model was the value of the F statistic. The classification model was constructed and optimized on a training set, while the test set, including data not included in the training process, was used to assess the effectiveness and predictive ability of the model. The next group consisted of separately selected kernels to check the correctness of the classification model.

Results and analysis

Whole grain – ventral side

Table 1 shows the results of the accuracy of classification of barley grains without segmentation into uniform areas for a wavelength of 600 nm (ventral side of the grain). The accuracy of the classification of infected grains was 48%, while for the wavelength of 800 nm the correctness of classification improved significantly and amounted to 95% (Tab. 2).

Table 1

Results of the correctness of grain classification for the whole grain with a wavelength of 600 nm, ventral side

Group	Classification [%]	B_V_600_WG [pcs]	M_V_600_WG [pcs]	H_V_600_WG [pcs]
B_V_600_WG	88	36	4	1
M_V_600_WG	48	10	20	12
H_V_600_WG	79	1	8	33

B_V_600__WG – black-tipped kernels – ventral side – 600 nm whole grain; M_V_600__WG – mold-affected kernels – ventral side – 600 nm whole grain; H_V_600__WG – healthy kernels – ventral side – 600 nm whole grain

Table 2

Results of the correctness of grain classification for the whole grain with a wavelength of 800 nm, ventral side

Group	Classification [%]	B_V_800 _WG [pcs]	M_V_800_WG [pcs]	H_V_800_WG [pcs]
B_V_800_WG	95	39	2	0
M_V_800_WG	98	1	41	0
H_V_800_WG	88	4	1	37

B_V_800 – black-tipped kernels – ventral side – 800 nm whole grain; M_V_800 – mold-affected kernels – ventral side – 600 nm whole grain; H_V_800 – healthy kernels – ventral side – 800 nm whole grain

Segmented grain – ventral side

In the next step, the surface of the kernel was divided into 3 homogeneous areas, and then the texture was measured and the results were subjected to statistical analysis. The results of grain classification based on textures measured from the ventral side at a wavelength of 600 nm are presented in Table 3, and the results for the wavelength of 800 nm are shown in Table 4. Classification improvements (100% and 93%) were achieved for healthy grains scanned at 600 and 800 nm. Similar results were obtained for rained grains. However, the grains affected by the fungus were classified at 93% and 86% depending on the wavelength.

Table 3

Results of the correctness of grain classification for grain segmentation with a wavelength of 600 nm, ventral

Group	Classification [%]	B_V_600_SG [pcs]	M_V_600_SG [pcs]	H_V_600_SG [pcs]
B_V_600_SG	98	40	1	0
M_V_600_SG	93	3	39	0
H_V_600_SG	100	0	0	42

H_D_600_SG – healthy kernels-dorsal-side – 600 nm grain segmentation; B_V_600_SG – black--tipped kernels – ventral side – 600 nm grain segmentation; M_V_600_SG – mold-affected kernels – ventral side – 600 nm grain segmentation

Table 4

Results of the correctness of grain classification for grain segmentation with a wavelength of 800 nm, ventral side

Group	Classification [%]	B_D_800_WG [pcs]	M_D_800_WG [pcs]	H_V_800_WG [pcs]
B_V_800_SG	98	40	1	0
M_V_800_SG	86	4	36	2
H_V_800_SG	93	0	3	39

H_V_800_WG – healthy kernels – ventral side – 800 nm whole grain; B_D_800_WG – black-tipped kernels – dorsal side – 800 nm whole grain; M_D_800_WG – mold-affected kernels – dorsal side – 800 nm whole grain

Whole grain – dorsal side

Tables 5 and 6 present the results of the whole-grain analysis from measurements taken from the dorsal side, for wavelengths of 600 nm and 800 nm, respectively. The least accurately classified cases were obtained for the classification of infected grains, with 86% accuracy for the 600 nm wavelength and 76% for the 800 nm wavelength. The other groups, on the other hand, were classified correctly with over 90% accuracy.

Table 5

Results of the correctness of grain classification for the whole grain with a wavelength of 600 nm, dorsal side

Group	Classification [%]	B_D_600_WG [pcs]	M_D_600_WG [pcs]	H_D_600_WG [pcs]
B_D_600_WG	90	37	2	2
M_D_600_WG	86	3	36	3
H_D_600_WG	90	3	1	38

H_D_600_WG – healthy kernels – dorsal-side – 600 nm whole grain; B_D_600_WG – black-tipped kernels – ventral side – 600 nm whole grain; M_D_600_WG – mold-affected kernels – ventral side – 600 nm whole grain

Table 6

Results of the correctness of grain classification for the whole grain with a wavelength of 800 nm, dorsal side

Group	Classification [%]	B_V_800_WG [pcs]	M_V_800_WG [pcs]	H_V_800_WG [pcs]
B_D_800_WG	95	39	0	2
M_D_800_WG	76	5	32	5
H_D_800_WG	95	2	0	40

H_D_800_WG – healthy kernels – dorsal side – 800 nm whole grain; B_D_800_WG – black-tipped kernels – ventral side – 800 nm whole grain; M_D_800_WG – mold-affected kernels – ventral side – 800 nm whole grain

Segmented grain – dorsal side

Another method of analysis was based on the use of spectral data obtained from images of grains after segmentation from the dorsal side for wavelengths of 600 nm (Tab. 7) and 800 nm (Tab. 8). The classification accuracy for this method was over 90% in both cases. Rainy grain analyzed from the dorsal side for a wavelength of 600 nm was correctly classified 100% of the time.

Table 7

Results of the correctness of grain classification for grain segmentation with a wavelength of 600 nm, dorsal side

Group	Classification [%]	B_V_600_SG [pcs]	M_V_600_SG [pcs]	H_D_600_SG [pcs]
B_D_600_SG	100	41	0	0
M_D_600_SG	94	0	17	1
H_D_600_SG	85	0	3	18

H_D_600_SG – healthy kernels – dorsal side – 600 nm grain segmentation; H_D_600_SG – healthy kernels – dorsal side – 600 nm grain segmentation; M_V_600_SG – mold-affected kernels – ventral side – 600 nm grain segmentation

Table 8

Results of the correctness of grain classification for grain segmentation with a wavelength of 800 nm, dorsal side

Group	Classification [%]	B_V_800_SG [pcs]	M_V_800_SG [pcs]	H_D_800_SG [pcs]
B_V_800_SG	95	39	1	1
M_V_800_SG	88	5	37	0
H_D_800_SG	93	1	2	39

H_D_800_SG – healthy grains – 600 nm grain segmentation dorsal side; H_D_800_SG – 800 nm grain segmentation dorsal side; M_V_800_SG – grains affected by mold – ventral 800 nm grain segmentation lateral side

Whole grain – dorsal and ventral side

A dataset was analyzed, in which the experimental group included textures obtained from the entire grain surface, without pagination, for wavelengths of 600 nm (Tab. 9) and 800 nm (Tab. 10). However, this type of approach resulted in a lower classification efficiency, which was only 60% for the 800 nm and 600 nm wavelengths. A particular difficulty was the classification of infected grains, with the correct distinction ranging from 59% to 69%. This result is consistent

Table 9

The results of the correctness of grain classification for the entire grain with a wavelength of 600 nm, without division into sides

Grupa	Klasyfikacja [%]	B_600_WG [pcs]	M_600_WG [pcs]	H_600_WG [pcs]
B_600_WG	93	38	3	0
M_600_WG	69	6	29	7
H_600_WG	81	0	8	34

H_600_WG – healthy kernels – 600 nm whole grain; B_600_WG – black-tipped kernels – 600 nm whole grain; M_600_WG – mold-affected kernels – 600 nm whole grain

Table 10

The results of the correctness of grain classification for the entire grain with a wavelength of 800 nm, without division into sides

Group	Classification [%]	B_600_WG [pcs]	M_600_WG [pcs]	H_600_WG [pcs]
B_800_WG	83	34	3	4
M_800_WG	60	7	25	10
H_800_WG	64	5	10	27

H_800_WG – healthy kernels – 800 nm whole grain; B_600_WG – black-tipped kernels – 800 nm whole grain; M_800_WG – mold-affected kernels – 800 nm whole grain

with observations, since fungal hyphae are most often present on the side of the sulcus, which is characterized by a specific folded structure, conducive to the colonization of fungal spores. The highest classification accuracy was recorded for depressed grains, regardless of wavelength. This is justified by the fact that the dark tips occur symmetrically on both sides of the grain, which makes it easier to identify and classify them with satisfactory efficiency.

Segmented grain – dorsal and ventral sides

Table 11 shows the results of grain classification after segmentation into the 600 nm wavelength without pagination. In the experimental system, the classification error was 2% for the irrigated grains. In the case of infected grains, the error was 21%, with 9 kernels being wrongly assigned to a different group. The results of classification accuracy for grains scanned at 800 nm are shown in Table 12. The highest number of incorrectly classified grains was obtained for grain infected with the fungus (18 cases of misclassification). Rained grains were classified with an accuracy of 90%.

Table 11

Results of the correctness of grain classification for grain segmentation with a wavelength of 600 nm, without division into sides

Group	Classification [%]	B_600_SG [pcs]	M_600_SG [pcs]	H_600_SG [pcs]
B_600_SG	95	39	1	1
M_600_SG	79	4	33	5
H_600_SG	76	0	10	32

H_600_SG – healthy kernels – 600 nm grain segmentation; B_600_SG – black-tipped kernels – 600 nm grain segmentation; M_600_SG – mold-affected kernels – 600 nm grain segmentation

Table 12

Results of the correctness of grain classification for grain segmentation with a wavelength of 800 nm, without division into sides

Group	Classification [%]	B_800_SG [pcs]	M_800_SG [pcs]	H_800_SG [pcs]
B_800_SG	90	37	3	1
M_800_SG	57	10	24	8
H_800_SG	74	6	5	31

H_800_SG – healthy kernels – 800 nm grain segmentation; B_800_SG – black-tipped kernels – 800 nm grain segmentation; M_800_SG – mold-affected kernels – 800 nm grain segmentation

Grain after segmentation – division into groups

The last analyzed dataset was constructed in such a way that each side of the grain was treated as a separate dataset, regardless of whether they were healthy, rainy, or fungus-infested grains. In this way, a database divided into 6 experimental groups was created. Table 13 shows the accuracy results of the

Table 13

Grain classification accuracy results for grain segmentation with a wavelength of 800 nm, whole grain

Group	Classification [%]	B_D_800_WG [pcs]	B_V_800_WG [pcs]	M_D_800_WG [pcs]	M_V_800_WG [pcs]	H_V_800_WG [pcs]	H_D_800_WG [pcs]
B_D_800_WG	100	41	0	0	0	0	0
B_V_800_WG	100	0	41	0	0	0	0
M_D_800_WG	100	0	0	42	0	0	0
M_V_800_WG	100	0	0	0	42	0	0
H_V_800_WG	100	0	0	0	0	42	0
H_D_800_WG	100	0	0	0	0	0	42

H_V_800_WG – healthy kernels – ventral side – 800 nm whole grain; H_D_800_WG – healthy kernels – dorsal side – 800 nm whole grain; B_D_800_WG – black-tipped kernels – dorsal side – 800 nm whole grain; B_V_800_WG – black-tipped kernels – ventral side – 800 nm whole grain; M_D_800_WG – mold-affected kernels – dorsal side – 800 nm whole grain; M_V_800_WG – mold-affected kernels – ventral side – 800 nm whole grain

Table 14

Grain classification accuracy results for grain segmentation with a wavelength of 600 nm, whole grain

Group	Classification [%]	B_D_600_WG [pcs]	B_V_600_WG [pcs]	M_D_600_WG [pcs]	M_V_600_WG [pcs]	H_V_600_WG [pcs]	H_D_600_WG [pcs]
B_D_600_WG	95	39	0	0	0	1	1
B_V_600_WG	80	1	33	1	2	0	4
M_D_600_WG	67	0	6	28	0	5	3
M_V_600_WG	76	0	4	0	32	0	6
H_V_600_WG	74	7	0	4	0	31	0
H_D_600_WG	60	0	8	4	5	0	25

H_V_600_WG – healthy kernels – ventral side – 600 nm whole grain; H_D_600_WG – healthy kernels – dorsal side – 600 nm whole grain; B_D_600_WG – black-tipped kernels – dorsal side – 600 nm whole grain; B_V_600_WG – black-tipped kernels – ventral side – 600 nm whole grain; M_D_600_WG – mold-affected kernels – dorsal side – 600 nm whole grain; M_V_600_WG – mold-affected kernels – ventral side – 600 nm whole grain

segmented grain classification for the 800 nm wavelength. This method allowed for a 100% correct classification of cases in the experimental group. However, for the 600 nm wavelength (Tab. 14), the classification error increased significantly, ranging from 5% to 40% depending on the experimental group.

Summary of results

The best identification of individual experimental groups of grains was obtained for the method using grain segmentation at a wavelength of 800 nm, taking into account both sides of the kernel. This method allowed for 100% correct classification. The graphical distribution of cases is shown in the scatterplot (Fig. 8).

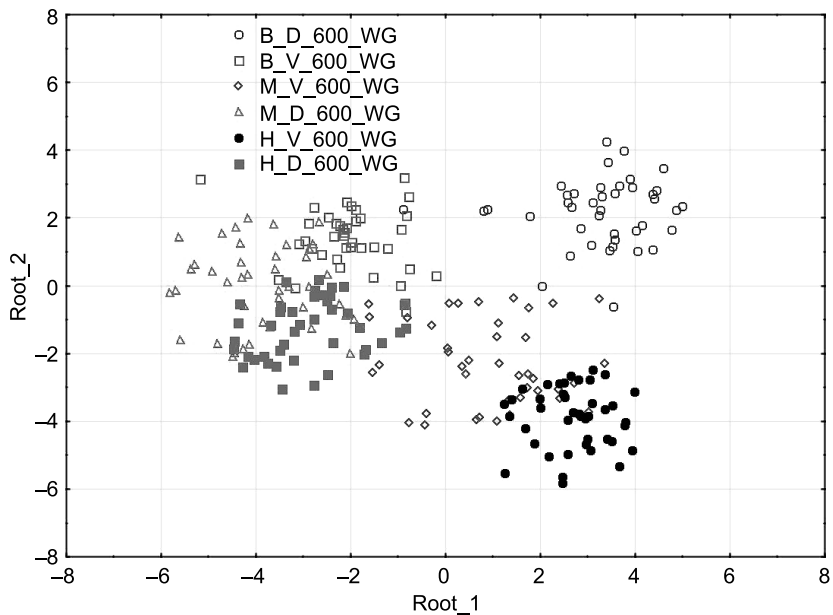

Fig. 8. Scatterplot of cases for individual experimental groups

The largest classification error was observed when analyzing the whole grain without prior segmentation, at a wavelength of 600 nm, where 26% of the samples were misclassified. To minimize classification errors in experimental groups, it is recommended to segment the grain into three homogeneous areas, which allows to achieve 100% correct classification. Scanning the grain from the furrow side is crucial as it minimizes the risk of classification errors. This is probably due to the fact that the furrows provide a favorable environment for the establishment

and development of fungal spores, which makes them more characteristic for the purposes of analysis. In addition, the recommended wavelength is 800 nm, as it allows for an improvement in classification accuracy of about 10% compared to images obtained at 600 nm, indicating a higher diagnostic value of this spectral range.

Conclusion

1. Images obtained at 800 nm showed the highest precision in the classification of experimental groups, while images taken at 600 nm showed an average of 10% greater classification error.

2. The use of segmentation of the kernel surface image allowed for a significant improvement in the accuracy of sample classification, indicating the importance of the analysis of isolated areas.

3. The highest classification accuracy was obtained by analyzing the textures coming from the grain furrow, where the percentage of correctly classified samples ranged from 94% to 98%, which emphasizes the importance of this specific surface in the classification process.

4. The best classification results were achieved using methods that allow the selection of 10 key variables for each qualitative group, which indicates their high diagnostic value in distinguishing individual classes.

5. Future studies should significantly increase the number of samples analysed and optimise the number of variables to further improve classification performance. It is also advisable to conduct comparative studies for other barley varieties to verify the versatility and effectiveness of the proposed method.

References

BAURIEGEL E., GIEBEL A., GEYER M., SCHMIDT U., HERPPICH W. 2011. *Early detection of Fusarium infection in wheat using hyper-spectral imaging*. Computer and Electronics in Agriculture, 75(2): 304-312. https://doi.org/10.1016/j.compag.2010.12.006

COGDILL R.P., HURBURGH C.R., RIPPKE G.R., BAJIC S.J.R., JONES W., MCCLELLAND J.F.T., JENSEN C., LIU J. 2004. *Single-kernel maize analysis by near-infrared hyperspectral imaging*. Transactions of the ASAE, 47(1): 311-320. https://doi.org/10.13031/2013.15856

DELWICHE S.R., KIM M.S. 2000. *Hyperspectral imaging for detection of scab in wheat*. In: *Biological Quality and Precision Agriculture II*. Eds. J.A. DeShazer, G.E. Meyer. Proceedings Volume, 4203. Environmental and Industrial Sensing. https://doi.org/10.1117/12.411752

DELWICHE S.R., KIM M.S., DONG Y. 2010. *Damage and quality assessment in wheat by NIR hyperspectral imaging*. In: *Sensing for agriculture and food quality and safety II*. Eds. M.S. Kim, S.-I. Tu, K. Chao. Proceedings Volume, 7676. SPIE Defense, Security, and Sensing. https://doi.org/10.1117/12.851150

DELWICHE S.R., KIM M.S., DONG Y. 2011. *Fusarium damage assessment in wheat kernels by Vis/NIR hyperspectral imaging*. Sensing and Instrumentation for Food Quality and Safety, 5(2): 63-71. https://doi.org/10.1007/s11694-011-9112-x

DOWELL F.E., RAM M.S., SEITZ L.M. 1999. *Predicting scab, vomitoxin, and ergosterol in single wheat kernels using near-infrared spectroscopy*. Cereal Chemistry, 76(4): 573-576. https://doi.org/10.1094/CCHEM.1999.76.4.573

GĄSIOROWSKI H. 1997. *Jęczmień. Chemia i technologia*. Wyd. I. Państwowe Wydawnictwo Rolnicze i Leśne, Poznań.

GIROLAMO A. DE, LIPPOLIS V., NORDKVIST E., VISCONTI A. 2009. *Rapid and non-invasive analysis of deoxynivalenol in durum and common wheat by Fourier-Transform Near Infrared (FT-NIR) spectroscopy*. Food Additives & Contaminants. Part A. Chemistry, Analysis, Control, Exposure and Risk Assessment, 26(6): 907-917. https://doi.org/10.1080/02652030902788946

NG H.F., WILCKE W.F., MOREY R.V., LANG J.P. 1998. *Machine vision evaluation of corn kernel mechanical and mold damage*. Transactions of the ASAE, 41(2): 415-420. https://doi.org/10.13031/2013.17166

PEARSON T.C., WICKLOW D.T. 2006. *Detection of corn kernels infected by fungi*. Transactions of the ASABE, 49(4): 1235-1245. https://doi.org/10.13031/2013.21723

POLDER G., HEIJDEN G.W.A.M. VAN DER, WAALWIJK C., YOUNG I.T. 2005. *Detection of Fusarium in single wheat kernels using spectral imaging*. Seed Science & Technology, 33(3): 655-668. https://doi.org/10.15258/sst.2005.33.3.13

SINGH C.B., JAYAS D.S., PALIWAL J., WHITE N.D.G. 2012. *Fungal damage detection in wheat using short-wave near-infrared hyperspectral and digital colour imaging*. International Journal of Food Properties, 15(1): 11-24. https://doi.org/10.1080/10942911003687223

SINGH C.B., JAYAS D.S., PALIWAL J., WHITE N.D.G. 2007. *Fungal detection in wheat using near-infrared hyperspectral imaging*. Transactions of the ASABE, 50(6): 2171-2176. https://doi.org/10.13031/2013.24077

TADEUSIEWICZ R., KOROHODA P. 1997. *Komputerowa analiza i przetwarzanie obrazów*. Wydawnictwo Fundacji Postępu Telekomunikacji, Kraków.

THOMAS S., WAHABZADA M., KUSKA M.T., RASCHER U., MAHLEIN A.K. 2017. *Observation of plant–pathogen interaction by simultaneous hyperspectral imaging reflection and transmission measurements*. Functional Plant Biology, 44(1): 23-34. https://doi.org/10.1071/FP16127